Física de la Tierra
2002, 14, 161-182

ISSN: 0214-4557

THE CORNER FREQUENCIES, STRESS DROPS AND APPARENT STRESSES OF MICROEARTHQUAKES IN THE BETIC REGION (SOUTHERN SPAIN)

J. M. García-García, M. D. Romacho and A. Jiménez
Departamento de Física Aplicada, Universidad de Almería, 04120 Almería, Spain

ABSTRACT

A collection of ground motion recordings has been obtained in the period 1988-1990. Data from the Betic region (southern Spain) have been analysed to study the source scaling. This data set includes records of 43 microearthquakes registered by short-period seismic stations of the RSA network, located around the Granada basin. At high frequencies, the spectrum of P and S waves is characterized by a trend of exponential decay, $e^{-\pi\kappa f}$. The κ parameter ranges, for all the stations, roughly from 0.01 to 0.04 sec for P-waves and from 0.006 to 0.04 sec for S-waves. Fluctuations were found to be randomly distributed, with no dependence on magnitude. The expected increase of κ versus hypocentral distance is not evident for these data, possibly due to the lack of information for distances greater than approximately 50 km and also the large fluctuations. Measurement uncertainties and high variability among the geomorphological features of the station sites are probably responsible for the observed dispersion. Spectral parameters were automatically determined by the methods of Snoke (1987) and Andrews (1986) and were analysed with respect to the source model of Brune (1970, 1971). The seismic moments (from P- and S- waves) ranged from 5.45×10^{17} to 1.53×10^{20} dyne cm. The mean ratio between $f_c(P)$ and $f_c(S)$ was found to be 1.3. The source radii spanned from 0.13 to 0.4 km and the static stress drop varied from 0.05 to 3.6 bars. Also, we have estimated the parameter ε (Zúñiga, 1993) to investigate possible variations in stress drop mechanism, and we have found a value of 0.6, which may be indicative of a partial stress release.

1. INTRODUCTION

The Granada basin, an intramountain neogene basin delimited and crossed by faults, is located in the central part of the Betic Cordilleras. The basin is post-tectonic in nature and structured from the upper Miocene to the present. Three fundamental sets of large faults oriented N70-100E, N120-150E and N10-70E, respectively, are present in the zone (Vidal, 1986; Peña et al., 1993). The epicentral distributions show that the seismic activity trends mainly in N40-60W and N20-30E, orientations well correlated with existing faults in this area.

The Central zone of the Betics has a high level of seismic activity. In the Granada basin, the earthquakes of 1431, 1806 and 1884 generated ground motions that reached intensity IX (MSK scale). Last century, two earthquakes generated intensity VIII, the events of 1910 (Santa Fé) and 1956 (Albolote). The main seismic activity of the Central Betic region is shallow, but there is a significant number of subcrustal events with depths down to 120 km (mainly in the south of Málaga) and there is also a very deep and rare seismic activity shown by 1954, 1973, 1990 and 1993 earthquakes with depths around 630-650 km. The Andalusian Seismic Network (Red Sísmica de Andalucía, RSA) has permitted since 1983 the analysis of several thousands of microearthquakes of the Granada basin.

The spectral analysis for the determination of source parameters, for microearthquakes and small earthquakes recorded with a local seismic network, has been widely used by different authors following Brune's (1970, 1971) and Boatwright's (1980) models and methods (see García-García *et al*., 1996b). This study presents a data set of source parameters and the scaling relations among them for microearthquakes occurring in the Granada basin, for which we have spectrally analysed 43 events using RSA digital data.

The relevant historic earthquakes that occurred between the 15th and 19th centuries (12 strong events with a maximum intensity of IX, MSK) are evidence of the importance of seismicity in the Betic region. During the last century, there has only been moderate seismic activity in this region, though some earthquakes have caused damage, but none with an intensity greater than VIII. Two earthquakes reached a magnitude greater than 6.0, namely the one of 16-June-1910 near Adra, (Almería) with a magnitude of 6.3 and the one of 29-March-1954 at Dúrcal (Granada) with a depth of 630 km and a magnitude of 7.0.

2. DATA

The data of this study were recorded by 8 short period seismic stations of the RSA network (Fig. 1), located around the Granada basin (Alguacil *et al*., 1990). All the stations were in a low-noise environment and all the geophones used had vertical component with 1 Hz natural period. Each channel signal was recorded in analog form and converted to digital form at a frequency of 100 Hz with a resolution of 12 bits. The sites of the stations are of hard bedrock. The 43 events were selected on the basis of a good signal to noise ratio, accurate epicentral location, no saturation of signal record and a suffici ent separation between P and S phases.

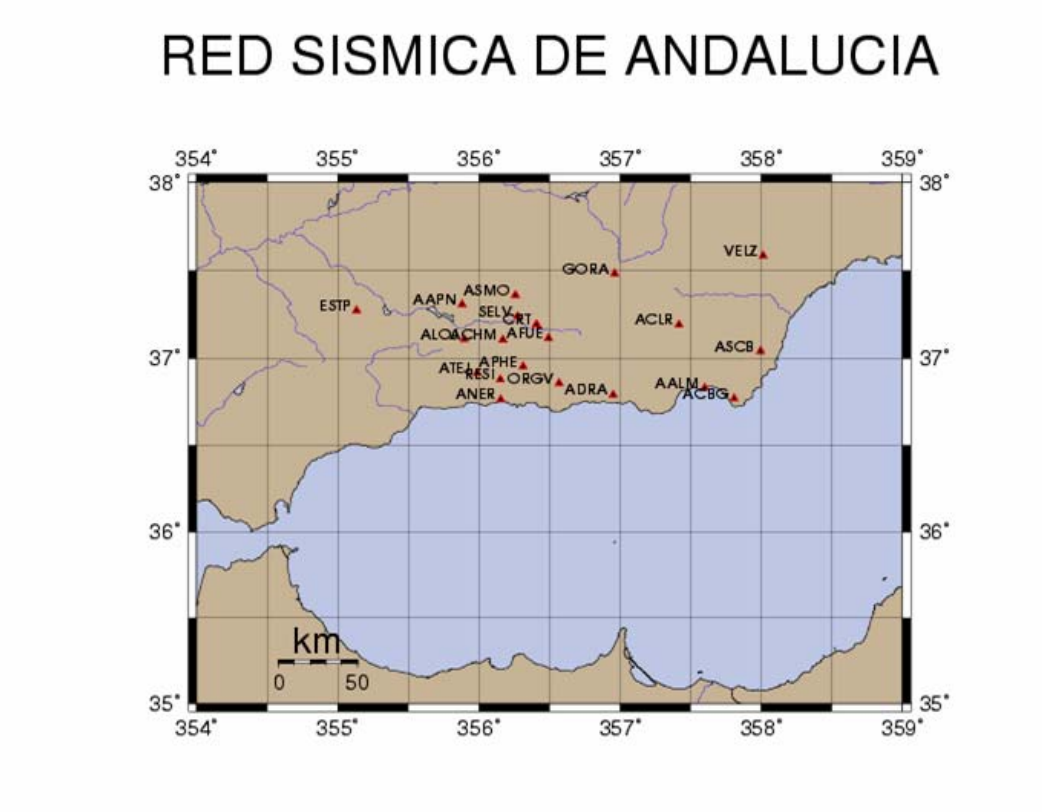

Figure 1. The RSA network.

The duration magnitude M_D of the selected events (Miguel *et al*., 1988) ranges between 1.4 and 3.5, corresponding to a moment magnitude M_w (Hanks and Kanamori, 1979) between 1.1 and 2.7. The hypocentral locations were revised using all the seismic stations of the Andalusian Seismic Network. Almost all the epicentres are in the Granada basin (Fig. 2), and the majority of them have a depth of less than 25 km (generally between 9 and 16 km).

All the data selected had a high quality with a characteristic impulsive P and S wave arrivals. The signal to noise spectral ratio was found to be greater than two orders of magnitude in the 1.0 to 20 Hz band for almost all the studied events.

The focal depth of these events is less than 25 km, except three which have a depth of between 40 and 60 km.

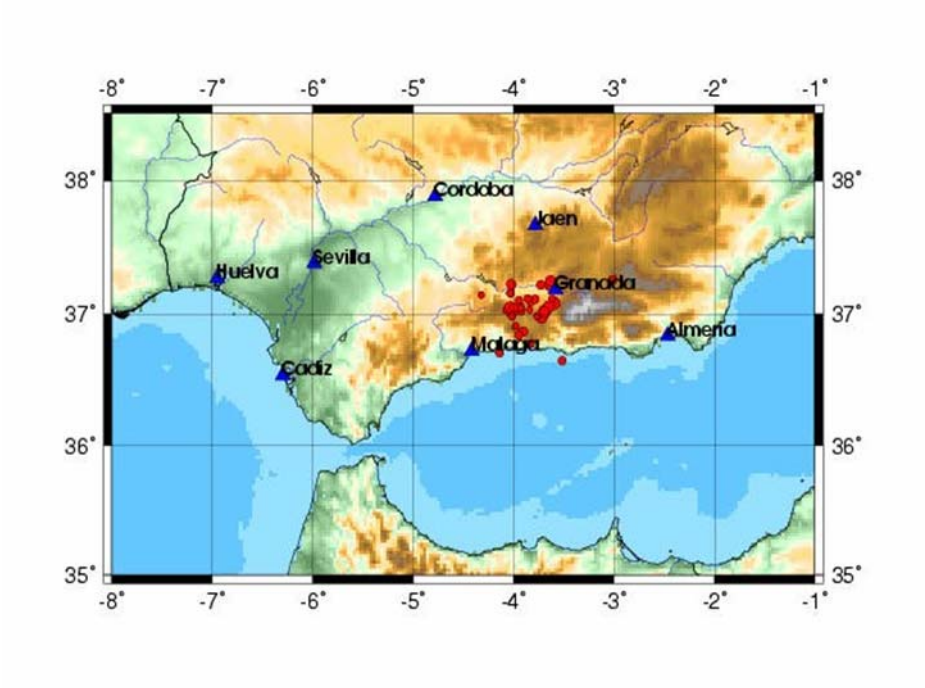

Figure 2. Map including the epicenters of the 43 events analysed (●), the size of the symbol is proportional to the magnitude.

3. THE SPECTRAL ANALYSIS AND THE SOURCE PARAMETERS.

Before calculating amplitude spectra, via the Fourier Transform, the signal was base-line corrected by removing the mean and the time series were windowed, for each phase, using a two-sided 10% cosine taper.

The theoretical spectrum may be described as: $R(f)=CI(f)S(f)D(f)$. The scaling factor C accounts for the effects of free surface correction (F) and by the rms average radiation model R_{2N}. S(f) is the source spectrum. We assumed a T-squared model for P- and S- waves for the ground displacement at the source. The spectra were corrected for instrumental response (I(f)), attenuation and site response. D(f) is the diminution function. The path-dependent part of the diminution function applied to the spectra corresponds to the anelastic attenuation correction $e^{+\pi f R/(Q(f)v(P,S))}$, with *Q(f)* being the quality factor, v(P,S) the velocities of P- or S- waves, respectively, and R the epicentral distance. R corrects the amplitude decay due to geometrical spreading and for body waves it is assumed to be 1/R (R< 100 km). The *coda-Q* values, Q_c (Ibáñez *et al*., 1990, 1991), were used instead of the Q_β values and the Q_α adopted was *(9/4)* Q_c (Burdick, 1978). The Q_c values employed were $Q_c = Q_0 f^{n}$, with Q_0 = 80 - 120 and n = 0.6 - 0.8. The near site attenuation has been accounted for by $e^{+\pi \kappa f}$ (Anderson and Hough, 1984; Bindi *et al*., 2001). The κ parameter was obtained at each station by fitting a straight line to the natural logarithm of the Fourier amplitude spectrum plotted as a linear function of frequency (García-García, 1995).

The κ parameter ranges, for all the stations, roughly from 0.01 to 0.04 sec for P-waves and from 0.006 to 0.04 sec for S-waves. Margaris and Boore (1998) examined sites for the determination of $\Delta\sigma$ and κ_0 from large earthquakes in Greece. They assigned each site to one of three classes- B, C and D. That classification relies on the shear-wave velocity averaged over the top 30 m (V_{30} greater than 750 m/sec for B, between 360 and 750 m/sec for C, and between 180 and 360 m/s for D). Margaris and Hatzidimitriou (2002) obtained a mean of κ_0- value of 0.035 for class B sites that correspond to hard rock. That is similar to the average κ_0 of 0.02 sec that we have obtained over all the analysed stations. The fluctuations were found to be randomly distributed, with no dependence on magnitude (Fig. 3a). The expected increase of κ versus hypocentral distance (Fig. 3b) is not evident for these data, possibly due to the lack of information for distances greater than some 50 km and also the large fluctuations. Measurement uncertainties and high variability among the geomorphological features of the station sites are probably responsible for the observed dispersion.

The model of Brune (1970, 1971) and the modified version of the spectral shape proposed by Boatwright (1980) were fitted to displacement spectra of P- wave and S- wave. The version of Boatwright (1980) produces a sharper corner shape than Brune's original model and a better match to the data, so it is consequently preferred in this study; similar appreciations are also found in Abercrombie (1995).

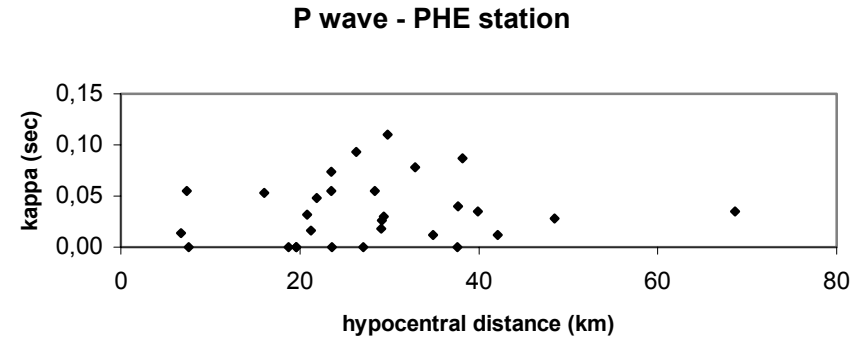

(a)

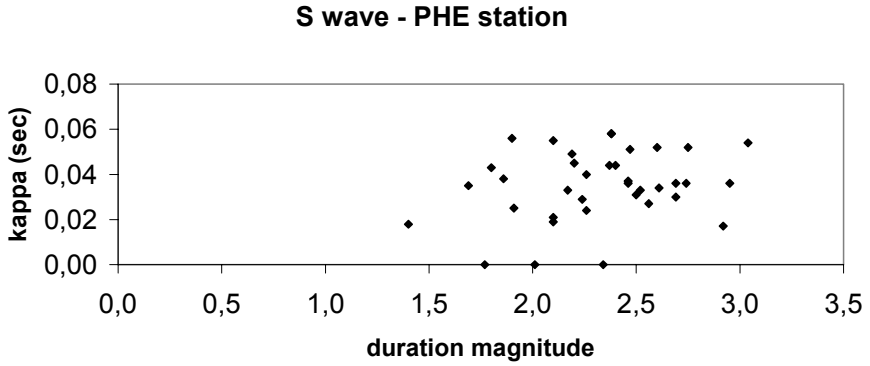

(b)

Figure 3. κ dependence on hypocentral distance (a), and magnitude (b).

Source parameters from the displacement spectra have been interpreted in the context of Brune´s source model with the low frequency level (Ω_0) and the corner frequency (f_c) being the usual spectral parameters.

To avoid problems associated with the visual determination of the corner frequency, f_c, we adopted the method of Snoke (Snoke, 1987). This method uses two independent parameters, the low frequency plateau, Ω_0, and the energy flux, J. Ω_0 is calculated by visual inspection of the displacement spectrum, whereas J is the integral of the square of the ground velocity of either P- or S- waves. The corner frequency is finally obtained as:

$$\left(\frac{J}{2\pi^3 \Omega_0^{\,2}} \right)^{1/3} \tag{1}$$

Also we compared these values with those obtained by Andrews' method (Andrews, 1986), according to the formula

$$\frac{1}{2\pi} \sqrt{\frac{\int_0^\infty V^2(f)\,df}{\int_0^\infty D^2(f)\,df}} \tag{2}$$

where V(f) and D(f) are the velocity and displacement spectra, respectively. Both determinations give almost the same results, indicating the high quality of the analysed data set and that the corrections applied to the spectra were adequate to obtain reliable source parameters. Average values for Ω_0 and fc from P, S waves and an average of (P, S) were obtained for each of the 43 events analysed. The logarithmically averaged ratio of the P-wave corner frequency to the S-wave corner frequency is 1.3. This result is similar to the average ratio of 1.1 obtained by Boatwright *et al.* (1991), analysing the recordings from 28 earthquakes ranging in size from M_D = 2.1 to 4.6. That result confirms the very common seismological observation that the P waveform is enriched in high-frequency motion relative to the S waveforms of the same earthquake (Hanks, 1981). In Fig. 4, the dashed lines on the plot show $f_c(P) = f_c(S)$ and $f_c(P) = (\alpha/\beta) f_c(S)$. The corner frequencies plotted in this figure are generally intermediate to these bounds.

Brune's (1970, 1971) fault model formulae were used for estimating seismic moment M_0, source radius r and stress drop $\Delta\sigma$. The average values were estimated following the method of Archuleta *et al*. (1982), where a multiplicative error factor is taken into account. For the seismic energy error factor, we used Scherbaum and Kisslinger's (1984) formulae. Table 1 gives the average values (from P and S waves) of M_0 , r, $\Delta\sigma$ and σ_{ap}, with their error factors, and the seismic energy E_S. The errors are not shown when the values are very small or estimated using only one station.

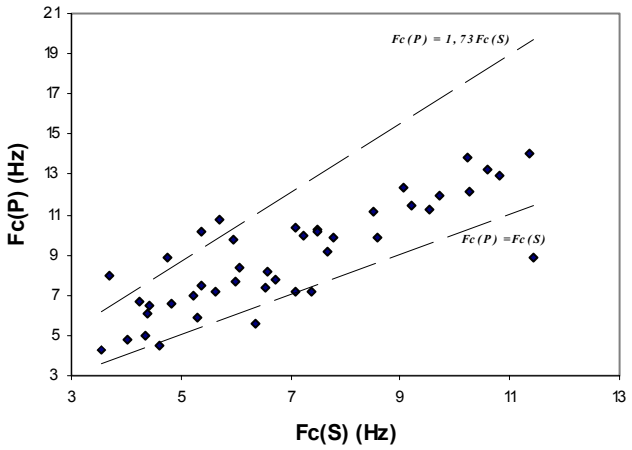

Figure 4. P-corner frequencies F_c(P) versus S-corner frequencies F_c(S). The dashed lines indicate an equal ratio F_c(P)/ F_c(S).

We have calculated the seismic moments M_0, for P- and S- waves by Snoke's method (determined from the long period part of the seismic spectrum) and also by Andrew's method. The results obtained are very similar. The seismic moments (Snoke's method) range from 5.45 x 10^{17} to 1.53 x 10^{20} dyne-cm. In Figure 5 we present the correlation between P- and S-wave results for M_0, with a correlation coefficient of 0.98. The logarithmic average $M_0(S)/M_0(P)$ is *0.9*. The agreement between seismic moments from P and S waves provides enough confidence that the source and attenuation parameters have been calculated with some precision, because they were

determined from different sets of spectral values (Fletcher and Boatwright, 1991).

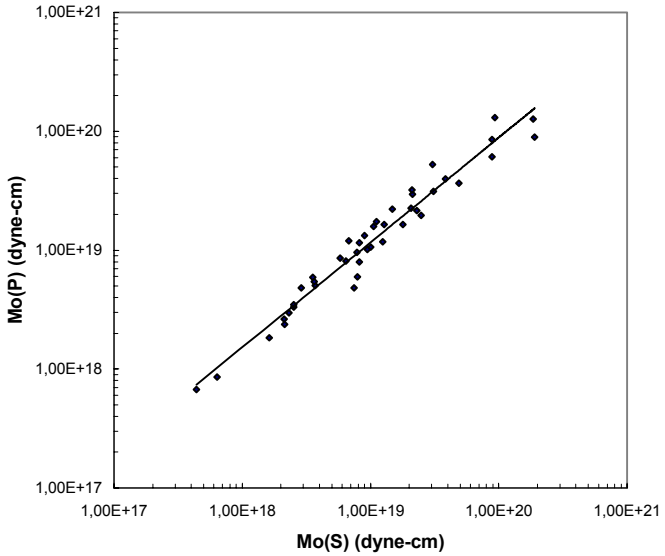

Figure 5. Correlation between P-and S- wave results for M_o. The straight line represents a least square linear fit.

The radiated seismic energy E_s of S-wave (or P-wave) was computed following Boatwright and Fletcher (1984):

$$E_S = \frac{4\pi\rho c R^2 J}{(F\Re_{\theta,\phi})^2} \qquad (3)$$

where Δ is the density (2.7 gr/cm^3); c represents either the shear velocity of 3.4 km/s or the compressional wave velocity of 6 km/s (Zappone *et al*., 2000); R is the hypocentral distance; $\Re_{2,N}$ is the radiation pattern coefficient for the S- or P- wave (Boore and Boatwright, 1984); F is the wave amplification

factor at the free surface. We have assigned an average value of 1, for both S- and P- wave (García-García *et al*., 1996a).

The seismic energies of P and S varies from 7.17 x 10^3 to 1.13 x 10^8 **J.** Seismic energy is plotted in Figure 6. We present the lines of equal energy ratio $E_S(P)/E_S(S)$; this ratio is found to be between 0.1 and 1 for about 81.4% of the events; the mean geometric $E_S(S)$ to $E_S(P)$ ratio is 5.5, similar to that obtained by Fletcher and Boatwright (1991) but almost half the value determined by Boatwright *et al*. (1991).

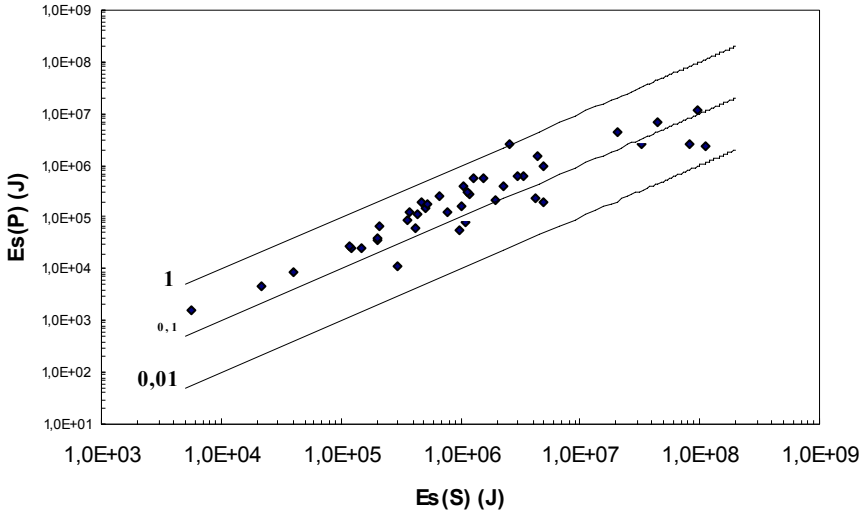

Figure 6. P-wave energy $E_S(P)$ versus S-wave energy $E_S(S)$. The lines indicate the ratio $E_S(P)/E_S(S)$ constant.

Generally, the stress state is characterized by implementing more than one stress parameter (Anderson, 1997; Margaris and Hatzidimitriou, 2002). In this study we analysed the conventional Brune stress drop and the apparent stress drop (σ_{ap}). The basic definition of σ_{ap} was proposed by Wyss (1970) as:

$$\sigma_{ap} = \mu \frac{E_s}{M_0} \qquad (4)$$

Where μ is the shear modulus (3.10^{10} N/m^2) and E_S is the total radiated seismic energy. This definition does not require any high-frequency decay assumption and does not depend on the source model, because it is obtained directly from seismic energy and seismic moment and they are only very slightly influenced by the source geometry.

The stress drops varies from 0.05 to 3.6 bars. The average value on the Brune stress drop is equal to 0.4 bars with an error factor of 2.3. Most of the apparent stress ranges from 0.04 to 6.4 bars and the mean value is equal to 0.4 bars with an error factor of 2.7. In Figure 7 we displayed the apparent stress versus stress drop and the least squares linear fit gives

$$\log \Delta\sigma_{ap} = (1.07 \pm 0.015) \log \Delta\sigma + (0.02 \pm 0.02) \qquad (5)$$

with a correlation coefficient (c.c.) of 0.95. As the slope of the fit line is almost one, it indicates that the original values of the variables are linearly correlated.

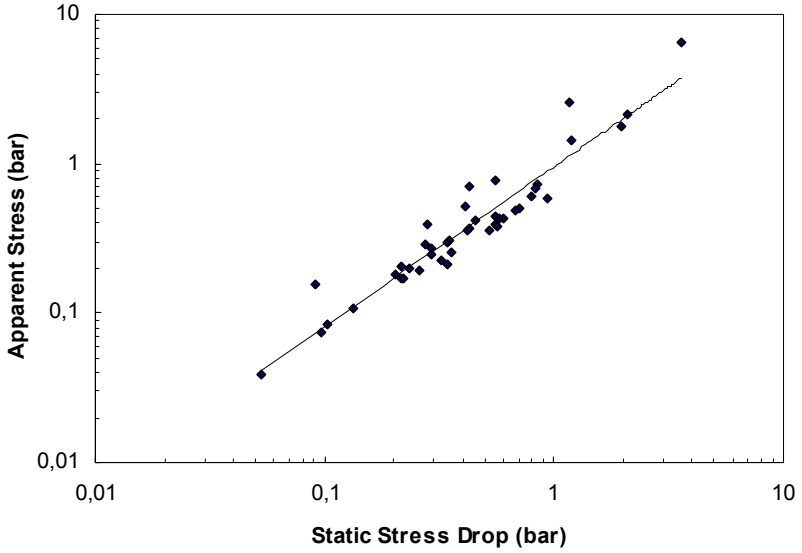

Figure 7. Apparent stress versus stress drop and the least squares line fit.

Zuñiga (1993) proposed, to investigate possible variations in stress drop mechanism, the use of the parameter ε, defined as

$$\varepsilon = \frac{\sigma_1 - \sigma_2}{\sigma_1 - \sigma_f} \qquad (6)$$

Here σ_1 and σ_2 are initial and final stresses and σ_f the frictional stress. This ratio provides an estimate of the amount of partial stress drop (the final stress is greater than the frictional stress on the fault) or frictional overshoot (the final stress reaches a value less than the frictional stress on the fault). We have obtained one value for ε of 0.6, which may be indicative of a partial stress release.

4. SCALING LAWS

Whereas the magnitude scales suffer severe intrinsic limitations, such as saturation and discrepancies between scales, the seismic moment (a measure of earthquake size defined in terms of parameters of the double-couple shear dislocation source model) can be estimated from the recordings of all suitable seismographs (Bakun, 1984). That is why it is usual to find empirical formulae relating the seismic moment with the magnitude.

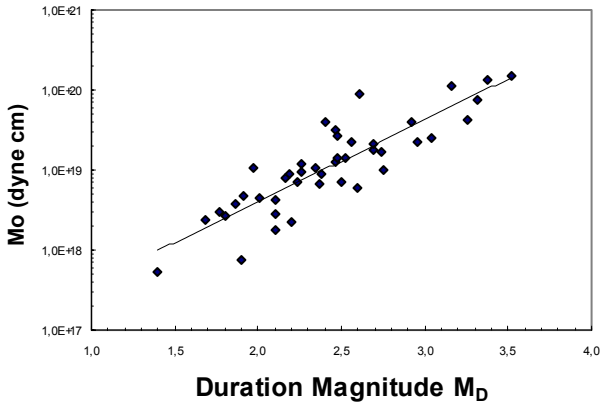

Figure 8. Plot of the seismic moment M_o, as determined from P- and S-waves, against duration magnitude M_D. The straight line represents the least squares fit to the data.

These expressions take the form of a linear relation between log M_0 and duration magnitude. In Figure 8 we have plotted log seismic moment against the duration-magnitude (M_D). A least squares fit to all data yields:

$$\log M_0 (P, S) = (1.02 \pm 0.09) M_D + (16.56 \pm 0.22) \quad (7)$$

with a c. c. of 0.87.

Scale invariance of the seismic rupture process is equivalent to the observation that the ratio of seismic moment to event radius is a power law with exponent 3 and the earthquakes have a constant stress drop. It has been observed in some studies that for events with $M_0 < 10^{20}$ dyne-cm, there is evidence for breakdown in constant stress drop scaling. In that case, the events appear to have a minimum source dimension of a few hundred meters and stress drop appears to decrease with decreasing seismic moment (Abercrombie and Leary, 1993). The relation between M_0 and stress drop $\Delta\sigma$ is shown in Fig. 9. Linear least squares fit through the data gives:

$$\log M_0 (P, S) = (1.10 \pm 0.17) \log \Delta\sigma + (19..47 \pm 0.09) \quad (8)$$

with a c.c. of 0.72.

In Figure 10 we plot seismic moment versus radius with lines of constant stress drop. The linear least squares fit through the data gives:

$$\log M_0 (P, S) = (3.28 \pm 0.43) \log r + (21.15 \pm 0.28) \quad (9)$$

Relations (8) and (9) indicate that our data are close to the limit where decreasing $\Delta\sigma$ with M_0 decreasing begins, and this suggests a breakdown in the similarity of rupture processes for the earthquakes studied here (García, 1995).

The values of the total seismic energy are plotted against the seismic moment in Figure 11. The values are bounded by lines of constant apparent stress to show that energy can vary for a given seismic moment. The geometric mean of E_S / M_0 is 1.2×10^{-6}; Kanamori (1977), following Orowan's model (1960), obtained a ratio of 5×10^{-5} for large earthquakes.

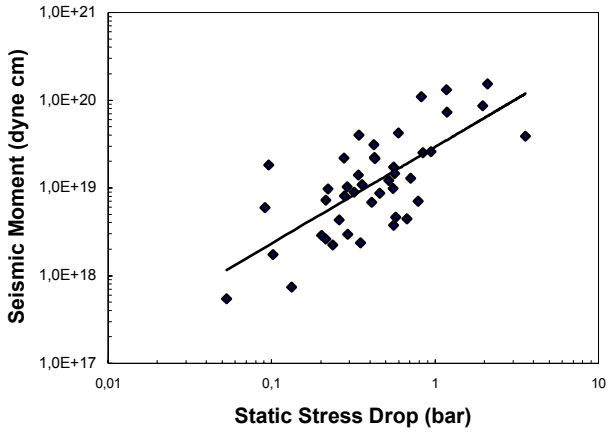

Figure 9. Relation between seismic moment M_o and static stress drop $\Delta\sigma$, as calculated from P- and S- waves. The straight line is the best fit to the data.

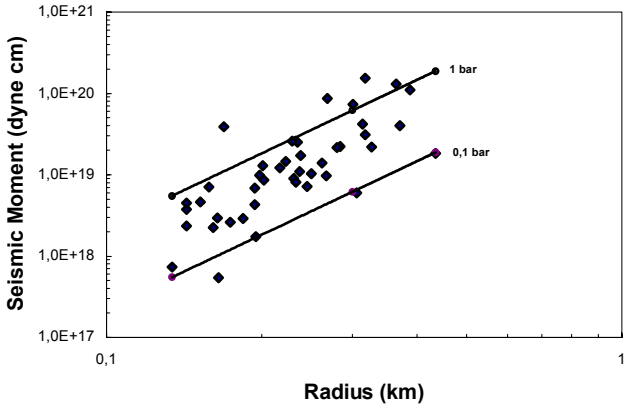

Figure 10. Seismic moment M_o plotted as a function of source radius r, as determined from P- and S- waves. The straight lines are contours of constant stress drop.

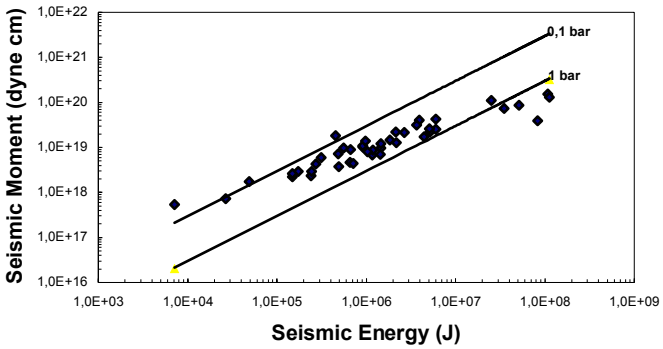

Figure 11. Total seismic energy E_s versus seismic moment M_o, as evaluated from P- and S- waves. The lines of constant apparent stress show the range of energy variation for a given seismic moment.

The M_w magnitude can be easily calculated using the standard formula of Hanks and Kanamori (1979), $M_W = (2/3)\log M_0 - 10.7$. We have also plotted the duration magnitude M_D against moment magnitude M_w (Fig. 12). A least squares fit to all data yields

$$M_W\ (P, S) = (0.69 \pm 0.07)\, M_D + (0.43 \pm 0.24) \qquad (10)$$

with a c.c. of 0.91. There is a good correlation between the duration magnitude and moment magnitude. Oncescu *et al*. (1994) obtained, for the spectra of 18 aftershocks of the M_L 5.8 Roermond earthquake, a similar ratio (with a slope of 0.68) between M_w and the local magnitude M_L.

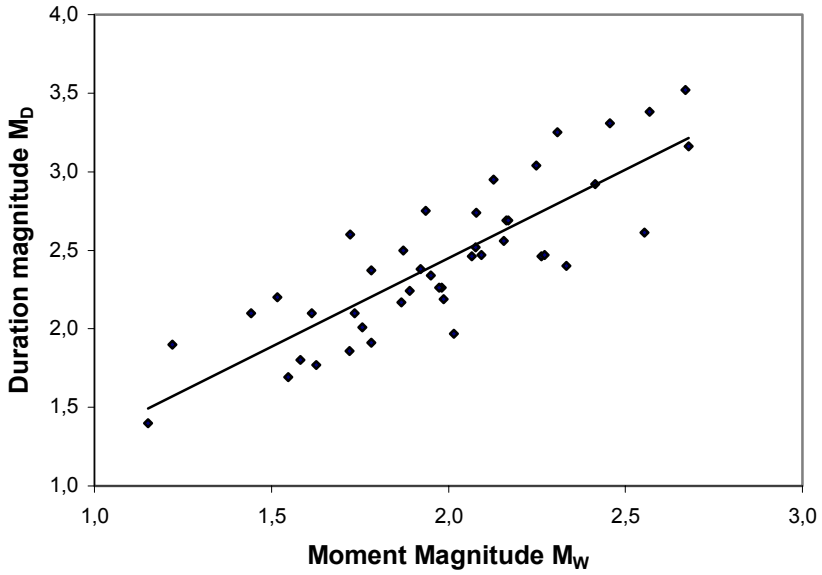

Figure 12. Correlation between moment magnitude M_w and duration magnitude M_D. A least squares linear fit has been applied to the data.

5. CONCLUSIONS

The events analysed here have proven to be a good set of digital data for estimating spectral and source parameters in this region. Our inversion of digital seismograms for 43 selected earthquakes recorded by 8 stations of the Andalusian Seismic Network has removed site and attenuation effects in order to keep only the source properties in our study. The ray path attenuation was taken into consideration using the *coda-Q* instead of Q_β. *Coda-Q* frequency dependent was calculated for the region by Ibáñez *et al*. (1990, 1991). The site effects were minimized using the parameter κ with values mainly in the range of 0.01 to 0.04 sec for P-waves and from 0.006 to 0.04 sec for S-waves.

A key parameter in quantifying source spectra is the corner frequency. The corner frequencies range from 4 to 12.6 Hz. The P-wave corner frequency values are higher than the S-wave values and their ratio is 1.3, which agrees with the ratio found by Boatwright and Fletcher (1984).

The seismic moment M_0 estimated from either P- or S-waves is different and was found to be between 5.45 x 10^{17} and 1.53 x 10^{20} dyne-cm, values similar to those obtained by other authors for earthquakes in our range of magnitude. The $M_0(P)$ to $M_0(S)$ ratio is 1.1, indicating that the radiation pattern average correction coefficients applied to the data were the appropriate ones.

The source radius was found to range from 0.13 to 0.40 km. The source sizes estimated from P-waves were greater than those estimated from S-waves, by a ratio of about 1.3.

The seismic energies determined range from 7.17 x 10^{3} to 1.13 x 10^{8} J. We have found a large variation in seismic energy values for each value of the seismic moment. The seismic energy values obtained for S-waves were greater than the values for P-waves and for 81.4 % of the events this ratio was found to be between 0.1 and 1.0. If different constant values of F (free surface coefficient) and $Y_{\theta,\varphi}$ (radiation pattern coefficient) were applied to our data, the seismic energy values could be slightly affected by a constant value. Similarly, the stress release and apparent stress parameters could be affected by the use of different constant coefficients.

The stress drop values were below 4 bars, a result similar to those obtained by authors working with comparable seismic moments (e.g. Douglas and Ryall, 1972; Dysart *et al*. 1988; Fletcher *et al*., 1986). Although high values of stress drop correspond to the higher seismic moment values, is not entirely conclusive with only such a low number of earthquakes that a decreasing stress drop occurs with a decreasing seismic moment.

Most of the apparent stress values estimated ranged from 0.04 to 6.4 bars. We have obtained one value for ε of 0.6, which may be indicative of a partial stress release.

ACKNOWLEDGMENTS.

We thank F. Vidal, J.M. Martín-Marfil, A. Posadas and F. Luzón, colleagues of the University of Almería, whose comments and useful discussions at the various stages of this study led to an improvement of the work. This work was partially supported by CICYT, Spain, under Grant REN2002-04198-C02-02/RIES, by the European Community with FEDER, by the research team of *Geofísica Aplicada* (RNM194) of Junta de Andalucía, by the Andalusian Institute of Geophysics and the University of Almería.

Table 1. N = event number; M_0 = average seismic moment (dyne cm); EM_0 = multiplicative error factor for M_0; r = average source radius (km); Er = multiplicative error factor for r; $\Delta\sigma$ = average stress drop; $E\Delta\sigma$ = multiplicative error factor for $\Delta\sigma$; σ_{ap} = average apparent stress; $E\sigma_{ap}$ = multiplicative error factor for σ_{ap}; E_S = average seismic energy; EE_S = multiplicative error factor for E_S; mgD = duration magnitude.

N	Mo	EMo	r	Er	Δσ	EΔσ	σap	Eσap	Es	EEs	mgD
26	5,99E+18	2,127	0,306	1,058	0,091	2,493	0,156	4,645	3,11E+05	2,184	2,6
37	2,89E+18	1,277	0,184	1,171	0,202	1,762	0,179	1,744	1,73E+05	1,365	2,1
39	7,37E+17	1,634	0,134	1,778	0,133	3,735	0,109	2,94	2,67E+04	1,799	1,9
43	4,31E+18	1,534	0,194	1,417	0,26	2,383	0,191	2,974	2,74E+05	1,938	2,1
44	5,45E+17	1,288	0,165	1,474	0,053	2,681	0,039	2,479	7,17E+03	1,925	1,4
46	2,24E+18	2,069	0,161	1,633	0,236	1,152	0,197	3,011	1,48E+05	1,455	2,2
48	1,73E+18	2,151	0,195	2,017	0,102	3,177	0,085	3,905	4,89E+04	1,815	2,1
52	2,20E+19	1,392	0,327	1,795	0,277	1,897	0,291	2,265	2,14E+06	1,628	3,0
55	7,21E+18	1,629	0,245	2,436	0,215	4,194	0,203	3,194	4,87E+05	1,961	2,5
58	2,61E+18	1,654	0,174	2,208	0,215	1,793	0,171	2,111	1,49E+05	1,276	1,8
69	2,22E+19	2,345	0,284	2,317	0,426	3,318	0,701	6,003	5,20E+06	2,56	2,6
114	6,86E+18	1,127	0,194	2,826	0,411	1,653	0,512	2,044	1,17E+06	1,813	2,4
120	1,53E+20	1,512	0,318	2,307	2,093	3,307	2,12	2,825	1,08E+08	1,869	3,5
122	2,35E+18	1,552	0,143	3,119	0,35	2,076	0,307	2,04	2,41E+05	1,314	1,7
123	2,51E+19	1,241	0,235	3,215	0,842	2,436	0,716	2,249	5,98E+06	1,812	3,0
130	1,72E+19	1,819	0,238	2,407	0,557	2,679	0,778	3,591	4,47E+06	1,974	2,7
134	4,00E+19	1,669	0,371	1,95	0,342	2,004	0,295	3,015	3,93E+06	1,806	2,9
144	7,33E+19	1,818	0,301	2,229	1,182	3,648	1,431	3,203	3,50E+07	1,761	3,3
145	8,66E+18	1,42	0,202	2,104	0,458	2,059	0,411	2,487	1,19E+06	1,752	2,4
146	1,82E+19	1,867	0,435	2,248	0,096	2,237	0,075	3,329	4,53E+05	1,783	2,7
155	1,29E+19	1,415	0,201	2,315	0,71	2,278	0,5	2,167	2,16E+06	1,531	2,5
157	1,03E+19	1,269	0,25	2,692	0,29	2,1	0,267	1,887	9,13E+05	1,488	2,3
159	4,22E+19	1,368	0,314	2,616	0,599	1,959	0,425	2,041	5,98E+06	1,492	3,3

Table 1 Continuation.

N	Mo	EMo	r	Er	Δσ	EΔσ	σap	Eσap	Es	EEs	mgD
163	9,81E+18	1,416	0,198	2,404	0,554	3,258	0,445	2,995	1,46E+06	2,114	2,8
180	1,31E+20	2,027	0,365	2,374	1,175	1,963	2,594	3,378	1,13E+08	1,667	3,4
182	3,73E+18	1,725	0,143	2,118	0,556	2,657	0,398	3,035	4,95E+05	1,76	1,9
184	9,00E+18	1,379	0,231	2,56	0,32	1,691	0,222	2,305	6,66E+05	1,671	2,2
187	3,91E+19	1,428	0,169	3,345	3,566	2,815	6,407	3,29	8,34E+07	2,304	2,4
204	8,07E+18	1,752	0,233	2,471	0,279	2,363	0,388	2,927	1,04E+06	1,67	2,2
205	1,45E+19	1,6	0,223	2,327	0,568	2,266	0,383	2,546	1,84E+06	1,591	2,5
207	1,21E+19	1,58	0,217	2,405	0,52	2,472	0,362	2,541	1,45E+06	1,608	2,3
209	9,67E+18	1,608	0,267	2,696	0,222	2,187	0,172	3,158	5,54E+05	1,965	2,3
212	1,09E+19	1,914	0,237	2,69	0,357	1,745	0,251	3,355	9,13E+05	1,753	2,0
215	3,11E+19	1,293	0,318	2,714	0,423	2,19	0,354	2,119	3,67E+06	1,639	2,5
217	7,07E+18	1,193	0,158	3,188	0,79	1,63	0,61	1,518	1,44E+06	1,273	2,2
220	2,60E+19	1,393	0,229	2,756	0,944	1,838	0,588	1,762	5,11E+06	1,265	2,5
230	8,67E+19	1,567	0,268	3,583	1,959	3,173	1,783	2,686	5,15E+07	1,714	2,6
232	4,60E+18	1,458	0,152	2,679	0,576	1,658	0,428	2,087	6,57E+05	1,431	1,9
234	2,96E+18	1,386	0,164	3,449	0,293	1,621	0,248	1,529	2,44E+05	1,103	1,8
238	4,46E+18	1,896	0,143	3,223	0,672	1,616	0,48	2,626	7,14E+05	1,385	2,0
239	1,10E+20	1,245	0,388	4,138	0,827	3,064	0,682	2,893	2,51E+07	2,324	3,2
240	2,16E+19	1,703	0,28	2,409	0,429	2,679	0,372	4,305	2,68E+06	2,527	2,7
242	1,39E+19	1,901	0,262	2,923	0,34	3,245	0,212	4,588	9,85E+05	2,413	2,5

REFERENCES

ABERCROMBIE, R. E. (1995): «Earthquake source scaling relationships from -1 to 5 M_L using seismograms recorded at 2.5-km depth», *J. Geophys. Res*., **100**, No. B12, 24,015-24,036.

ABERCROMBIE, R. E. AND LEARY, P. C. (1993): «Source parameters of small earthquakes recorded at 2.5 km depth, Cajon Pass, southern California: implications for earthquake scaling», *Geophys. Res. Letts*.., **20**, 1511-1514.

ALGUACIL, G., GUIRAO, J. M., GÓMEZ, F., VIDAL, F. AND DE MIGUEL, F. (1990): «Red Sísmica de Andalucía (RSA): A digital PC-based seismic network», *Cahiers du Centre Européen de Géodynamique et de Séismologie,* **1**, 19-27.

ANDERSON, J. G. (1997): «Seismic energy and stress-drop parameters for a composite source model», *Bull. Seism. Soc. Am*., **87**, No. 1, 85-96.

ANDERSON, J. G. AND HOUGH, S. E. (1984): «A model for the shape of the Fourier amplitude spectrum of acceleration at high frequencies», *Bull. Seism. Soc. Am*., **74**, No. 5, 1969-1993.

ANDREWS, D. J. (1986): «Objective determination of source parameters and similarity of earthquakes of different size», *Proc. 5th Maurice Ewing Symp. Earthquake Source Mechanics*, S. Das. J. Boatwright and C. H. Scholtz editors, American Geophysical Union. Washington, D. C., 259-267.

ARCHULETA, R. J., CRANSWICK, E., MUELLER, CH. AND SPUDICH, P. (1982): «Source parameters of the 1980 Mammoth lakes, California, earthquakes sequence», *J. Geophys. Res.*, **87**, No. B6, 4595-4607.

BAKUN, W. H. (1984): «Seismic Moments, Local Magnitudes, and Coda Duration Magnitudes for Earthquakes in Central California», *Bull. Seism. Soc. Am*., **74**, 439-458.

BINDI, D., SPALLAROSSA, D., AUGLIERA, P., AND CATTANEO, M. (2001): «Source parameters from the aftershocks of the 1997 Umbria – Marche (Italy) seismic sequence», *Bull. Seism. Soc. Am*., **91**, 448-455.

BOATWRIGHT, J. (1980): «A spectral theory for circular seismic sources simple estimates of source dimension, dynamic stress drop, and radiated seismic energy», *Bull. Seism. Soc. Am.,* **70**, 1-26.

BOATWRIGHT, J. AND FLETCHER, J. B. (1984): «The partition of radiated energy between P and S waves», *Bull. Seism. Soc. Am*., **74**, No. 2, 361-376.

BOATWRIGHT, J., FLETCHER, J. B. AND FUMAL, T. E. (1991): «A general inversion scheme for source, site, and propagation characteristics using multiply recorded sets of moderate-sized earthquakes», *Bull. Seism. Soc. Am*., **81**, No. 5, 1754-1782.

BOORE, D. M. AND BOATWRIGHT, J. (1984): «Average body-wave radiation coefficients», *Bull. Seism. Soc. Am*., **74**, No. 5, 1615-1621.

BRUNE, J. N. (1970): «Tectonic stress and the spectra of seismic shear waves from earthquakes», *J. Geophys. Res.*, **75**, 4997-5009.

BRUNE, J. N. (1971): «Correction (to Brune (1970))», *J. Geophys. Res.*, **76**, 5002.

BURDICK, L. J. (1978): «t* for waves with a continental ray path», *Bull. Seism. Soc. Am*., **68**, No. 4, 1013-1030.

DOUGLAS, B. M. AND RYALL, A. (1972): «Spectral characteristics and stress drop for microearthquakes near Fairview Peak, Nevada», *J. Geophys. Res.*, **77**, No. 2, 351-359.

DYSART, P. S., SNOKE, J. A. AND SACKS, I. S. (1988): «Source parameters and scaling relations for small earthquakes in the Matsushiro region, southwest Honshu, Japan», *Bull. Seism. Soc. Am.*, **78**, No. 2, 571-589.

FLETCHER, J. B. AND BOATWRIGHT, J. (1991): «Source parameters of Loma Prieta aftershocks and wave propagation characteristics along the San Francisco Peninsula from a joint inversion of digital seismograms», *Bull. Seism. Soc. Am.,* **81**, No. 5, 1783-1812.

FLETCHER, J. B., HAAR, L.C., VERNON, F. L., BRUNE, J. N., HANKS, T. C. AND BERGER, J. (1986): «The effects of attenuation on the scaling of source parameters for earthquakes at Anza, California», In *Proc. 5th Maurice Ewing Symp. Earthquake Source Mechanics*, S. Das, J. Boatwright, and C. H. Scholtz editors, American Geophysical Union, Washington, D.C., 331-338.

GARCÍA-GARCÍA, J. M. (1995): *Características espectrales y de fuente de terremotos y microterremotos de Andalucía Orien*tal, PhD Thesis, Universidad de Granada.

GARCÍA-GARCÍA, J. M., VIDAL, F. ROMACHO, M. D., MARTÍN-MARFIL, J., POSADAS A. AND LUZÓN, F. (1996a): «Seismic Source Parameters for microearthquakes and small earthquakes of the Granada basin (Southern Spain)», *Tectonophysics*, **261**, 51-66.

GARCÍA-GARCÍA, J. M., ROMACHO, M. D., VIDAL, F., MARTÍN-MARFIL, J., POSADAS A. AND LUZÓN, F. (1996b): «Parámetros espectrales y fuente de los eventos de la serie sísmica de Adra-Berja (Almería), 1993-1994», *Libro Dedicado al Prof. Fernando De Miguel*, Universidad de Granada, 207-236.

HANKS, T. C. (1981): «The corner frequency shift, earthquake source models, and Q», *Bull. Seism. Soc. Am.,* **71**, No. 3, 597-612.

HANKS, T. C. AND KANAMORI, H. (1979): «A moment magnitude scale», *J. Geophys. Res.*, **84**, No. B5, 2348-2350.

IBÁÑEZ, J. M., DEL PEZZO, E., DE MIGUEL, F., HERRÁIZ, M., ALGUACIL, G. AND MORALES, J. (1990): «Depth-dependent seismic attenuation in the Granada zone (Southern Spain)», *Bull. Seism. Soc. Am.*, **80**, No. 5, 1232-1244.

IBÁÑEZ, J. M., DE MIGUEL, F., ALGUACIL, G., MORALES, J., VIDAL, F., DEL PEZZO, E. AND POSADAS, A. (1991): «Coda Q analysis of the digital data in the Central Betics», *Revista de Geofísica*, **47**, 59-74.

KANAMORI, H. (1977): «The energy release in great earthquakes», *J. Geophys. Res.*, **82**, 2981-2987.

MARGARIS, B. N. AND BOORE, D. M. (1998): «Determination of $\Delta\sigma$ and κ_0 from response spectra of large earthquakes in Greece», *Bull. Seism. Soc. Am.*, **88**, 170-182.

MARGARIS, B. N. AND HATZIDIMITRIOU, P. M. (2002): «Source Spectral Scaling and Stress Release Estimates Using Strong-Motion Records in Greece», *Bull. Seism. Soc. Am.*, **92**, 1040-1059.

MIGUEL, F. DE, ALGUACIL, G. AND VIDAL, F. (1988): «Una escala de magnitud a partir de la duración para terremotos del sur de España», *Revista de Geofísica*, **44**, 75-86.

ONCESCU, M. C., CAMELBEECK, T. AND MARTIN, H. (1994): «Source parameters for the Roermond aftershocks of 1992 April 13-May 2 and site spectra for P and S waves at the Belgian seismic network», *Geophys. J. Int.*, **116**, 673-682.

OROWAN, E. (1960): «Mechanism of seismic faulting», *Geological Society of America Memoirs*, **79**, 323-345.

PEÑA, J. A., VIDAL, F., POSADAS, A., MORALES, J., ALGUACIL, G., DE MIGUEL, F., IBÁÑEZ, J., ROMACHO M. D. AND LÓPEZ-LINARES, A. (1993): «Space clustering properties of the Betic-Alboran earthquakes in the period 1962-1989», *Tectonophysics,* **221**, 125-134.

SCHERBAUM, F. AND KISSLINGER, C. (1984): «Variations of apparent stresses and stress drops prior to the earthquake of 6 May 1984 (m_b = 5.8) in the Adak seismic zone», *Bull. Seism. Soc. Am.*, **74**, No. 6, 2577-2592.

SNOKE, J. A. (1987): «Stable determination of (Brune) stress drops», *Bull. Seism. Soc. Am.*, **77**, No. 2, 530-538.

VIDAL, F. (1986): *Sismotectónica de la región Béticas-Mar de Alborán*, Ph. D. Thesis. Universidad de Granada. Granada. 450 pp.

WYSS, M. (1970): «Stress estimates for South American shallow and deep earthquakes», *J. Geophys. Res.*, **75**, 1529-1544.

ZAPPONE, A., FERNANDEZ, M., GARCIA-DUEÑAS, V. AND BURLINI, L. (2000): «Laboratory measurements of seismic P-wave velocities on rocks from the Betic chain (southern Iberian Peninsula)», *Tectonophysics*, **317**, 259-272.

ZUÑIGA, F. R. (1993): «Frictional overshoot and partial stress drop. Which one?», *Bull. Seism. Soc. Am.*, **83**, No. 3, 939-944.